

Carbamylated erythropoietin mediates retinal neuroprotection in streptozotocin-induced early-stage diabetic rats

Xiaojing Liu · Bijun Zhu · Haidong Zou · Daode Hu ·
Qing Gu · Kun Liu · Xun Xu

Received: 15 July 2014 / Revised: 14 January 2015 / Accepted: 10 February 2015 / Published online: 1 March 2015
© Springer-Verlag Berlin Heidelberg 2015

Abstract

Purpose The neuroprotective effect of carbamylated erythropoietin (CEPO), an erythropoietin (EPO) derivative, in diabetic retinopathy (DR) has not been clearly verified. We conducted this study to investigate the potential neuroprotective role of CEPO in a streptozotocin-induced diabetic rat model.

Methods Streptozotocin-induced diabetic rats and blank controls were treated with or without CEPO and EPO for 4 weeks. Retinal functional and histological changes were quantified by electroretinogram, light microscopy, and terminal dUTP nick end labeling assay. Gene and protein levels of colony-stimulating factor 2 receptor beta, low-affinity (CD131), EPO receptor (EPOR), THY1, glial fibrillary acidic protein (GFAP), and vascular endothelial growth factor (VEGF-A) in retinal tissues were determined by real-time PCR and western blotting, respectively. Vascular penetration was assessed by fluorescein retinal angiography.

Results Diabetic rats had decreased retinal thickness, decreased ganglion cells, and increased retinal neuron apoptosis. CEPO increased CD131 and THY1 expression, while EPO increased EPOR expression. High glucose increased GFAP expression in the diabetic group, but both CEPO and EPO attenuated the trend for increase. CEPO downregulated VEGF-A expression. The amplitudes of b-wave and oscillatory potentials were decreased in the untreated diabetic group, whereas neither parameter decreased in diabetic rats after CEPO

or EPO treatment. Vascular leakage and microaneurysms in the diabetic group were significantly improved following CEPO treatment.

Conclusions CEPO has similar anti-apoptotic effects to EPO in DR, but CEPO does not induce neovascularization. CEPO may exert neuroprotective effects via its receptor CD131.

Keywords Carbamylated erythropoietin · Diabetic retinopathy · Retinal ganglion cells · Apoptosis · CD131

Introduction

Diabetic retinopathy (DR) is the most common complication of diabetes, and is the major cause of blindness in the working population in Western countries [1]. Most diabetic patients will develop varying degrees of DR [2]. Initially, DR was believed to be a type of microangiopathy caused by hyperglycemia. DR has become known as a disease induced by neural degeneration and which is manifested in the form of retinal ganglion cell (RGC) apoptosis and abnormal activation of glial cells prior to the occurrence of retinal microangiopathy [3, 4]. Currently, vascular endothelial growth factor (VEGF-A) antagonists are believed to inhibit the neovascularization of DR, but they damage the retinal neural tissues [5]. Therefore, the ideal treatment for DR should suppress microangiopathy and neuropathy in DR synchronously.

Mature erythropoietin (EPO) is a glycoprotein composed of 165 amino acids; it stimulates erythroid progenitor cell and early erythroblast maturation, and is mainly used in anemia treatment [6]. EPO also has neuroprotective functions [7]. EPO exerts different effects by binding to differently configured receptors. For example, EPO stimulates erythroid cell maturation by binding with a homodimer receptor. It can also suppress apoptosis and protect neural cells by binding to the heterodimer receptor colony-stimulating factor 2 receptor

X. Liu · B. Zhu · H. Zou · Q. Gu · K. Liu · X. Xu
Department of Ophthalmology, Shanghai First People's Hospital,
Shanghai Jiaotong University School of Medicine, Shanghai, China

D. Hu
Department of Pharmacology, Shanghai First People's Hospital,
Shanghai Jiaotong University School of Medicine, Shanghai, China

B. Zhu (✉)
Haining Road No. 100, Hongkou District, 200080 Shanghai, China
e-mail: judyzhu52@126.com

beta, low-affinity (CD131) [7]. EPO administered through the subcutaneous or peripheral veins can cross the retina to reach effective therapeutic concentrations and avoid complications such as hemorrhage and infection caused by intravitreal injection [8–10]. Via electroretinogram (ERG) examination in diabetic rats, we found that recombinant human EPO (rhEPO) prevented decreases of b-wave amplitude and oscillatory potentials (Ops), and decreased neural tissue damage in DR in an obvious manner [10]. However, the fact that EPO is an important angiogenesis growth factor restricts its application in ophthalmology.

Carbamylated EPO (CEPO), an EPO derivative, can specifically bind to CD131 and has the same neuroprotective effect as EPO. CEPO neuroprotection has been verified in animal models of cerebral ischemic stroke, sciatic nerve compression, spinal cord injury, experimental allergic encephalomyelitis, and diabetic neuropathy [11]. Moreover, CEPO does not bind to the classic EPO receptor (EPOR) or exhibit any hematopoietic activity [7]. CEPO can cross the blood–retinal barrier, and its receptor, CD131, is expressed in retinal tissue [11]. However, little is known of the exact role of CEPO in ocular diseases, especially DR. Therefore, we proposed the hypothesis that CEPO mediates retinal neuroprotection in DR.

Materials and methods

Preparation and identification of CEPO

CEPO was synthesized as described previously using rhEPO (Shenyang Sunshine Pharmaceutical Co., Ltd., Shenyang, China) [11]. Briefly, one volume of rhEPO (1 mg/ml) was mixed with one volume of 0.5 M sodium borate (pH 9.0), and then recrystallized potassium cyanate was added to make a final concentration of 1 M. The mixture was incubated at 37 °C for 16–24 hours. It was dialyzed immediately against Milli-Q water for at least 48 hours and subsequently against 20 mM sodium citrate in 0.1 M NaCl (pH 6.0) for at least 48 hours at 4 °C. After dialysis, proteins were quantified by Bradford protein assay, and the sample was concentrated to 1 mg/mL by Centricon filtration (Millipore, Billerica, MA, USA). CEPO was identified using chromatography. We added 20 µL sample (1 mg/ml) and 20 µL EPO separately into Tris solution (25 mM Tris–HCl [pH 8.5], 1 mM EDTA, 7 M urea) and then incubated them for 1 hour at 37 °C. Subsequently, the two solutions were added separately to dithiothreitol (DTT) to a final concentration of 5 mM DTT, and incubated for 20 minutes at 50–60 °C. The two solutions were cooled to room temperature and added to iodoacetamide to a final concentration of 15 mM iodoacetamide, and then left for 15 minutes at room temperature. These solutions were added to a HiTrap desalt column

(pre-balanced with 25 mM Tris–HCl [pH 8.5], 1 mM EDTA, 0.4 M urea) and the flow velocity was controlled at 0.8 ml/min before we collected the eluting peak. Enzyme digestion was carried out after two aliquots of 1 µl endoproteinase Lys-C (0.1 µg/µl) were added separately to the two 20-µl eluates described above and incubated for 20 hours at 37 °C. The molecular weight of the product was determined using sodium dodecyl sulfate–polyacrylamide gel electrophoresis (SDS-PAGE) and silver nitrate staining.

Experimental design and animal model

We purchased 120 male Sprague–Dawley rats weighing 180–200 g from the Shanghai Laboratory Animal Center of the Chinese Academy of Sciences (Shanghai, China). The animals were treated in accordance with the Association for Research in Vision and Ophthalmology Statement for the Use of Animals in Ophthalmic and Vision Research. Rats were supplied with food and water and allowed to adjust to the new environment for 2 weeks before they were assigned randomly to control and diabetic groups. Rats in the diabetic group received 60 mg/kg streptozotocin (STZ) solution intraperitoneally after a 12-hour fast. Blood samples were obtained from the caudal vein after 3 days and 1 week respectively. Random blood glucose >16.7 mM was considered to indicate successful construction of a diabetic model. The control group received the same volume of citrate–sodium citrate buffer (pH 4.5, 0.1 mol/l). We monitored the blood glucose of all rats once a week. Following the successful construction of the diabetic model, rats were assigned randomly to four subgroups ($n=30$ each): CON (only given sodium citrate), DM (untreated STZ-induced diabetic rats), DM+E (STZ-induced diabetic rats treated with 5000 IU/kg EPO intraperitoneally three times a week for 4 weeks beginning 4 weeks after diabetes induction), and DM+C (STZ-induced diabetic rats treated with 50 µg/kg CEPO intraperitoneally three times a week for 4 weeks beginning 4 weeks after diabetes induction).

After the 4 weeks, all rats underwent ERG and histopathological examination. The eyes were enucleated and dissected immediately under a stereomicroscope by blunt dissection. Six retinas per group were fixed in 4 % paraformaldehyde (PFA) for 24 hours at 4 °C. The fixed retinal tissues were embedded in paraffin, and 5-µm sections were cut through the optic disk. The sections were stained with hematoxylin and eosin, or processed for terminal deoxynucleotidyl transferase–mediated digoxigenin–dUTP nick end labeling (TUNEL). Another six retinas per group were frozen in liquid nitrogen and stored at –80 °C for western blotting and real-time PCR. The remaining rats were used for fluorescein retinal angiogram.

ERG examination

Four weeks after EPO or CEPO treatment, ERG (EP-1000; Tomey, Erlangen, Germany) was performed for each treatment group ($n=8$ per group). All examinations abided by the clinical standard ERG protocol (International Standardization Committee, 1989) [12]. Following dark adaptation overnight, all rats were anesthetized with an intraperitoneal injection of 1 % sodium pentobarbital (Sigma–Aldrich, St. Louis, MO, USA) under dim red illumination. Mydriasis was achieved with topical 0.5 % tropicamide (Santen Pharmaceutical, Osaka, Japan) for three times. Following topical anesthesia with 0.4 % oxybuprocaine hydrochloride eye drops (Santen Pharmaceutical), rats were stationed at a distance of 20 cm and facing the stimulus. Stainless steel wire loops (0.1-mm diameter) were placed on the center of the cornea after Vidisc gel (Bausch & Lomb, Rochester, NY, USA) was dropped in the conjunctival sac as a conducting medium. A reference electrode was placed in the middle of the lower eyelid, and a grounding electrode was placed near the tail. We used a black patch to cover the other eye during the experiment. Responses to a light flash (2.5 cd s/m^2) from a photic stimulator were amplified. Physioelectrical signals were impedance-matched through a unity gain preamplifier; preamplifier bandwidth was set at 0.3–300 Hz (maximal response) and 75–300 Hz (Ops). ERG analysis consisted of determining the amplitudes of a-wave, b-wave, and Ops, which were measured using a series of four bright white flashes at 15-second intervals [13]. Rats were kept warm with a heating pad throughout the experiment.

Histopathological examination

Retinal slices were stained with hematoxylin–eosin, and color micrographs were photographed at $400\times$ magnification under a light microscope (Leica, Heidelberg, Germany). The thicknesses of the total retina, inner plexiform layer (IPL), inner nuclear layer (INL), and outer plexiform (OPL) and outer nuclear layers (ONL) (referred to as the outer retinal layers, ORL) were measured at 0.5 mm dorsally and ventrally from the optic disc. The number of RGCs was calculated using the linear cell density (cells per $100 \mu\text{m}$). Three measurements at adjacent locations in each hemisphere were performed, and the average of nine measurements of three eyes was recorded as the representative value for each group.

Detection of retinal neuron apoptosis

3, 3'-Diaminobenzidine (DAB) TUNEL (Roche, Basel, Switzerland) was performed as described in the manual. Briefly, paraffin sections were prepared and subjected to TUNEL analysis after incubation with proteinase K and DAB. Following hematoxylin counterstaining, images were photographed

using a microscope at $100\times$ magnification. Apoptotic neurons within the retina were stained brown.

Real-time PCR

Total RNA was extracted from snap-frozen retinal tissues using the TRIzol method, and a DNase treatment step was included. We verified the absence of genomic DNA contamination of RNA samples by performing PCR using gene-specific primers designed using Primer Express software with published gene sequences. Table 1 lists the studied genes, primer sequences, and product sizes.

All gene transcripts were analyzed by quantitative PCR with SYBR Green Master Mix (ABI, Foster City, CA, USA) using an ABI PRISM 7900HT Sequence Detection System. Each sample was amplified in triplicate. Data were analyzed with SDS software (ABI). All assays were performed in triplicate. After an initial activation step at 50°C for 2 minutes and a hot start at 95°C for 5 minutes, PCR cycles consisted of 40 cycles at 95°C for 15 seconds, 55°C for 15 seconds, 72°C for 20 seconds, and 76°C for 3 seconds. Quantitative PCR product specificity was assessed routinely by performing a dissociation curve at the end of the amplification program. Gene expression was normalized using the mean β -actin gene expression from the same sample and calculated relative to controls using the relative standard curve method. Results were expressed as $2^{-\Delta\Delta\text{CT}}$ (CT, threshold cycle), as shown in Table 1.

Western blotting

Thawed retinas were sonicated in Tris-buffered saline (TBS) containing protease inhibitors and centrifuged to collect the supernatant ($14,000g$, 15 minutes, 4°C). Protein concentration was measured using a Bio-Rad Protein Assay kit (Hercules, CA, USA), and about $80 \mu\text{g}$ protein per lane was loaded and resolved with 10 % SDS-PAGE. The proteins of interest were transferred to polyvinylidene difluoride transfer membranes and blocked in TBST (0.05 % Tween and 5 % skimmed milk in TBS) for 2 hours at 4°C . The membranes

Table 1 Primer sequences used and their product sizes

Gene	Primer (forward, reverse; 3' to 5' end)	Product (bp)
<i>CD131</i>	CCATCTCGTGGTCCGCTGGC CCCCAAGGGGCACACTCCAC	110
<i>EPOR</i>	GGGACGCGTACACCTTCGC TCAGTAGCGACGCGGGCTCA	94
<i>VEGF-A</i>	TGTGAGCCTTGTTTCAGAGCGGA ACTCAAGCTGCCTCGCCTTGC	109
<i>THY1</i>	CACACTTACCGCTCCCGCGT GTCGCCCTCATCCTTGGTGGT	90
<i>GFAP</i>	TGACGCCTCCACTCCCTGCC CATCTCCGCACGCTCGCTGG	95

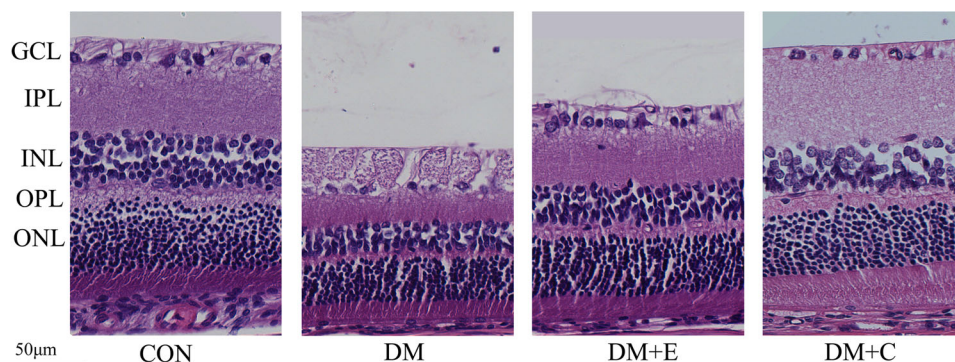


Fig. 1 Representative micrographs of the superior region of the retina after 4-week EPO or CEPO treatment. In the CON group, the structure of the GCL and INL was well-organized. Four weeks after diabetes induction, the INL in the DM group was obviously thinner, the number

of GCL cells had decreased, and vacuoles were visible in the RGC layer. Four weeks after EPO (DM+E) or CEPO (DM+C) treatment, the retinal structure appeared more normal, with a thicker INL than in the DM group, but the total retinal thickness was thinner. Scale bar: 50 μ m

were incubated with monoclonal antibodies against rat EPOR, CD131, VEGF-A, THY1, and glial fibrillary acidic protein (GFAP) at 1:1,000 dilutions overnight, rinsed in TBST, and then incubated for 1 hour with a secondary antibody against rabbit immunoglobulin G (1:5,000). After rinsing in TBST again, an enhanced chemiluminescence kit (Pierce, Rockford, IL, USA) was used to detect the blots, and the signals were quantified by densitometry. β -Actin expression (1:5,000; monoclonal anti- β -actin; Sigma–Aldrich) was used as the internal loading control to confirm equivalent total protein loading, and experiments were repeated in triplicate.

Fluorescein isothiocyanate–dextran retinal angiogram

Rats were anaesthetized using 10 % chloral hydrate, the thorax was opened, and the heart was exposed. We perfused through the left ventricle with 50 mg/ml high–molecular weight (2×10^6) fluorescein isothiocyanate–conjugated dextran (Sigma–Aldrich). The rats were immediately sacrificed by cervical dislocation, and the eyes were enucleated and

fixed in 4 % PFA for 12 hours at 4 °C. The lenses were then removed, and the retinas incised radially. After the vitreous humor was removed, the retinas were flat-mounted with an anti-fade kit (Beyotime, Shanghai, China). Retinal vessels were visualized by fluorescence microscopy and photographed with a digital camera (Axioplan 2 imaging E; Zeiss, Oberkochen, Germany).

Statistical analysis

All data are expressed as mean \pm standard deviation, and statistical calculations were performed using SPSS version 12.0 (SPSS, Chicago, IL, USA). Groups were tested for normal distribution using the Shapiro–Wilk test and for variance homogeneity using the Levene test. Differences between two paired data sets were compared using a 2-sample *t*-test, while unpaired groups were compared using analysis of variance (ANOVA). When the sample size was too small and did not accord with normal distribution, statistical comparisons between unpaired groups were performed using the Mann–

Table 2 Retinal thickness and RGC counts after 4-week treatment ($\bar{x} \pm s$)

Group (<i>n</i> =6 per group)	Thickness (μ m)				GCL cells (per 100 μ m)
	Total retina	IPL	INL	ORL	
CON	194.0 \pm 19.5	46.2 \pm 4.7	33.1 \pm 5.4	54.0 \pm 14.4	9.5 \pm 1.8
DM	137.9 \pm 14.1 ^{a*}	29.5 \pm 5.3 ^{a*}	23.8 \pm 3.2 ^{a*}	37.9 \pm 4.2 ^{a*}	5.1 \pm 1.5 ^{a*}
DM+E	181.3 \pm 11.7 ^{b*}	45.4 \pm 9.0 ^{b*}	26.7 \pm 2.3 ^{a*}	38.2 \pm 4.6 ^{a*}	8.8 \pm 2.0 ^{b*}
DM+C	198.8 \pm 15.8 ^{bc*}	60.8 \pm 6.2 ^{abc*}	34.5 \pm 3.9 ^{bc*}	48.5 \pm 5.8 ^{bc*}	8.5 \pm 1.7 ^{b*}
<i>F</i>	38.25	46.90	21.66	10.79	15.06
<i>P</i>	0.00	0.00	0.00	0.00	0.00

Values were compared between groups using 1-way ANOVA with LSD post-test. **p*<0.05

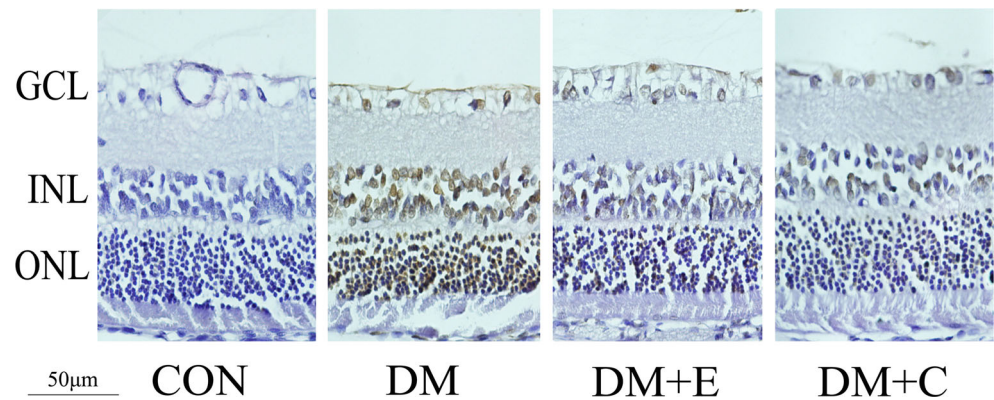
^a Compared with the CON group

^b Compared with the DM group

^c Compared with the DM+E group

GCL Ganglion cell layer

Fig. 2 Neuronal cell apoptosis detected by TUNEL after 4-week treatment. *Blue*: nuclear staining by hematoxylin; *brown*: DAB-stained apoptotic cells. There was no positive TUNEL staining in the GCL, INL, and ONL layers in the CON group, while there was much more staining in the DM group. However, there was less TUNEL staining in both the DM+E and DM+C groups than in the DM group. *Scale bar*: 50 μ m



Whitney test; that between paired groups were performed using Wilcoxon's test. All differences were considered significant at $p < 0.05$.

Results

Histopathological examination

Figure 1 depict the changes in the RGCs and ONL. RGCs from the diabetic rats had significant vacuolation, and the INL were swollen compared to that of the control rats. The RGCs from diabetic rats treated with EPO and CEPO did not have obvious vacuolation and a swollen INL layer, but the total retinal thickness became thinner (Fig. 1, Table 2).

Detection of retinal neuron apoptosis

Figure 2 illustrates the DAB staining of retinal neuronal apoptosis after the 4-week treatment. The retinal cell nuclei in the

Table 3 Apoptotic cell counts after 4-week treatments ($\bar{x} \pm s$) (per 100 μ m)

Group ($n=6$ per group)	GCL	INL	ONL
CON	1.25 \pm 1.00	2.17 \pm 1.60	18.67 \pm 2.57
DM	7.50 \pm 1.17a*	25.83 \pm 5.49a*	80.00 \pm 9.54a*
DM+E	5.08 \pm 1.88ab*	10.25 \pm 2.60ab*	47.83 \pm 5.73ab*
DM+C	3.67 \pm 1.50ab*	10.25 \pm 4.71ab*	39.75 \pm 4.48ab*
<i>F</i>	37.32	75.92	206.81
<i>P</i>	0.00	0.00	0.00

Values were compared between groups using 1-way ANOVA with Dunnett T3 post-test

* $p < 0.05$

^a Compared with the CON group

^b Compared with the DM group

^c Compared with the DM+E group

GCL Ganglion cell layer

CON group were negative for TUNEL staining, with no brown DAB coloring. There were abundant brown retinal neuronal nuclei in the INL and ONL, and RGCs in the DM group. By contrast, in the DM+E and DM+C groups, TUNEL revealed less retinal brown nucleic staining (Fig. 2, Table 3).

Gene expression in the retinas

EPO treatment significantly upregulated *EPOR* gene expression ($p < 0.05$, Fig. 3), while CEPO treatment did not induce a similar trend. Following CEPO treatment, the level of *CD131* gene expression was the same as that of the CON group ($p > 0.05$, Fig. 3), while *CD131* expression in the DM and DM+E groups was significantly downregulated.

Whether EPO and CEPO have retinal neuroprotective function was studied by measuring gene expression of the cytokine *THY1*. The level of *THY1* mRNA of rats in the DM, DM+E, and DM+C groups was downregulated compared to the CON group and only the data of the DM group were statistically significant compared to that of the CON group ($p < 0.05$, Fig. 3).

The activation of neural glial cells was measured by *GFAP* gene expression. Figure 3 shows that *GFAP* gene expression in the DM group was significantly upregulated compared to that of the CON group ($p < 0.05$), and that in the DM+E and DM+C groups was also upregulated but significantly lower than that in the DM group ($p < 0.05$).

After the 4-week treatments, *VEGFA* gene expression in the DM and DM+E groups was upregulated compared to that of the CON group ($p < 0.05$), but that in the DM+C group was not upregulated compared to that of the CON group ($p > 0.05$, Fig. 3).

Protein expression in the retinas

Whole-retina western blotting demonstrated that *EPOR* expression was significantly increased in the DM+E group; *CD131* expression was significantly increased in the DM+C group compared to that in the CON group ($p < 0.05$). *VEGFA* expression was upregulated in diabetic rats and EPO-treated diabetic rats, while CEPO administration did not upregulate *VEGFA* expression ($p < 0.05$). A marker of retinal neural

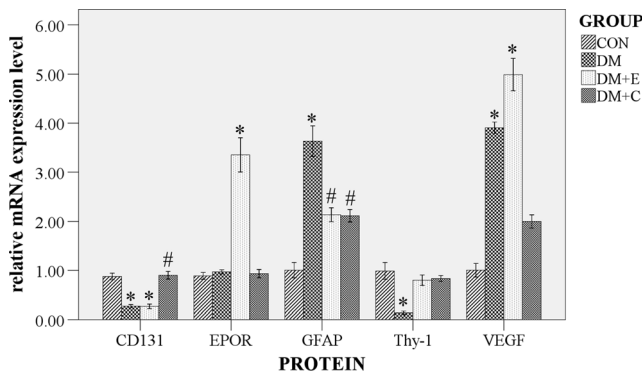


Fig. 3 *CD131*, *EPOR*, *GFAP*, *THY1*, and *VEGF-A* mRNA levels at 4 weeks after intervention. *GFAP* expression was highest in the DM group; *EPOR* and *VEGF-A* expression was highest in the DM+E group. *CD131* expression in the DM+C group was higher than that in the DM+E group. *THY1* expression in the DM+C group was higher than that in the DM group, but the same as that in the DM+E group. $n=6$ per group. * $p<0.05$ compared with CON group; # $p<0.05$ compared with DM group

protection, *THY1* expression was upregulated in EPO- and CEPO-treated diabetic rats in an obvious manner (Fig. 4, DM+E and DM+C groups) compared to that in untreated diabetic rats ($p<0.05$) (Fig. 4, DM group). *GFAP* expression in diabetic rats was increased compared to that of the controls, while EPO and CEPO administration reduced *GFAP* expression in diabetic rats significantly ($p<0.05$). Four weeks after EPO and CEPO treatment, *VEGF-A* expression in the DM and DM+E groups was upregulated compared to that of the CON group ($p<0.05$), as was that in the DM+C group ($p<0.05$), albeit less than that of the DM group ($p<0.05$, Fig. 4).

ERG

After the 4-week treatment, there was an obvious decrease in the b-wave amplitude of rats in the DM group compared to

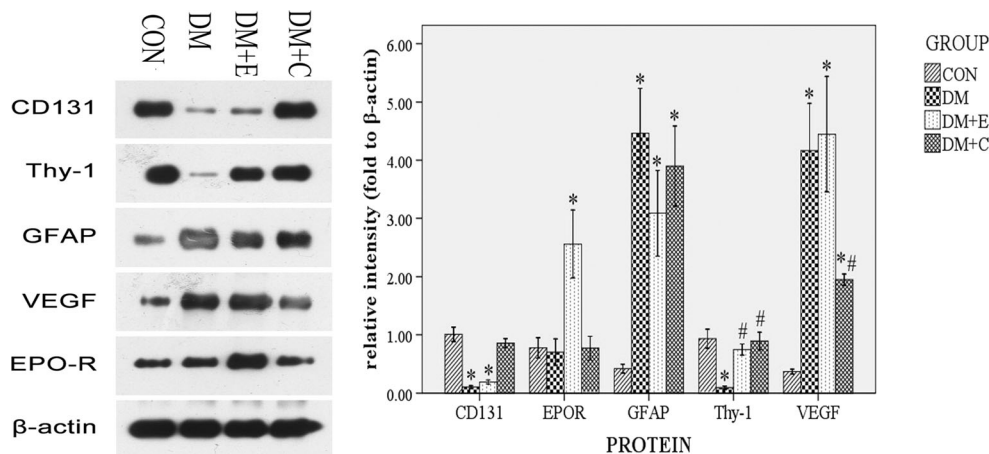


Fig. 4 Levels of *CD131*, *EPOR*, *GFAP*, *THY1*, and *VEGF-A* protein after 4-week treatment with EPO and CEPO. *GFAP* expression was highest in the DM group; *EPOR* and *VEGF-A* expression was highest in the DM+E group; *CD131* expression in the DM+C group was higher

than that in the CON group ($p<0.05$), but there was no significant difference between the CON, DM+E, and DM+C groups ($p>0.05$). There was an obvious decrease in the Ops amplitude of rats in the DM and DM+E groups if compared with rats of CON group ($p<0.05$). In the DM+C group, Ops amplitude was not decreased compared to the CON group, although it was higher than that in the DM group ($p<0.05$) (Fig. 5, Table 4).

Fluorescein retinal angiogram evaluation of CEPO in retinal penetration and angiogenesis

The retinal angiograms demonstrated that the retinal vessels of the control rats were normally distributed and that there was no obvious vascular distortion, expansion, or exudation of the deep vessels after the 4-week CEPO treatment (Fig. 6a and b). There were many microaneurysms in diabetic rat retinas, representing microvascular expansion, which were full of fluorescein exudation (Fig. 6c and d). The rat retinas developed similar microaneurysms and exudation following EPO administration (Fig. 6e and f), but did not have obvious vascular exudation, distortion, or expansion after CEPO administration (Fig. 6g and h).

Discussion

In this study, we showed that administering CEPO intraperitoneally in diabetic rats decreased RGC apoptosis and improved retinal function in DR as EPO did. Importantly, CEPO upregulated *CD131* expression but had no effect on *EPOR* expression in diabetic rats, suggesting that CEPO-induced neuroprotection is mediated through a *CD131*-dependent transduction mechanism.

than that in the DM+E group, and *THY1* expression was higher than that in the DM group, but the same as that in the DM+E group. $N=6$ per group. * $p<0.05$ compared with CON group; # $p<0.05$ compared with DM group

CEPO treatment greatly reduced the number of apoptotic RGCs, prevented further retinal thinning, upregulated THY1 expression, and halted the b-wave decrease in diabetic rats, suggesting that CEPO confers the same neuroprotection as EPO through an anti-apoptotic function in retinal neural cells in our DR model. It has been acknowledged that the main manifestations of DR are RGC apoptosis and abnormal activation of glial cells [14–17]. At the same time, the retinal IPL and INL thickness became thinner [14]. Therefore, protecting RGCs is vital for treating DR. Our previous research proved that rhEPO administered intraperitoneally improves the decreased b-wave and Ops amplitude in an obvious manner,

Table 4 Statistical analysis of maximal response and Ops of rat eyes after 4-week treatments (μv)

Group (n=6 per group)	a-wave	b-wave	Ops
CON	40.30±15.70	160.90±61.29	211.45±55.65
DM	34.78±7.52	47.60±33.01 ^{a*}	17.83±9.57 ^{a*}
DM+E	68.50±19.54	149.35±64.19 ^{b*}	84.48±26.05 ^{a*}
DM+C	63.80±14.11	132.18±13.16 ^{b*}	156.55±21.33 ^{b*}

* $p < 0.05$

^a Compared with the CON group

^b Compared with the DM group

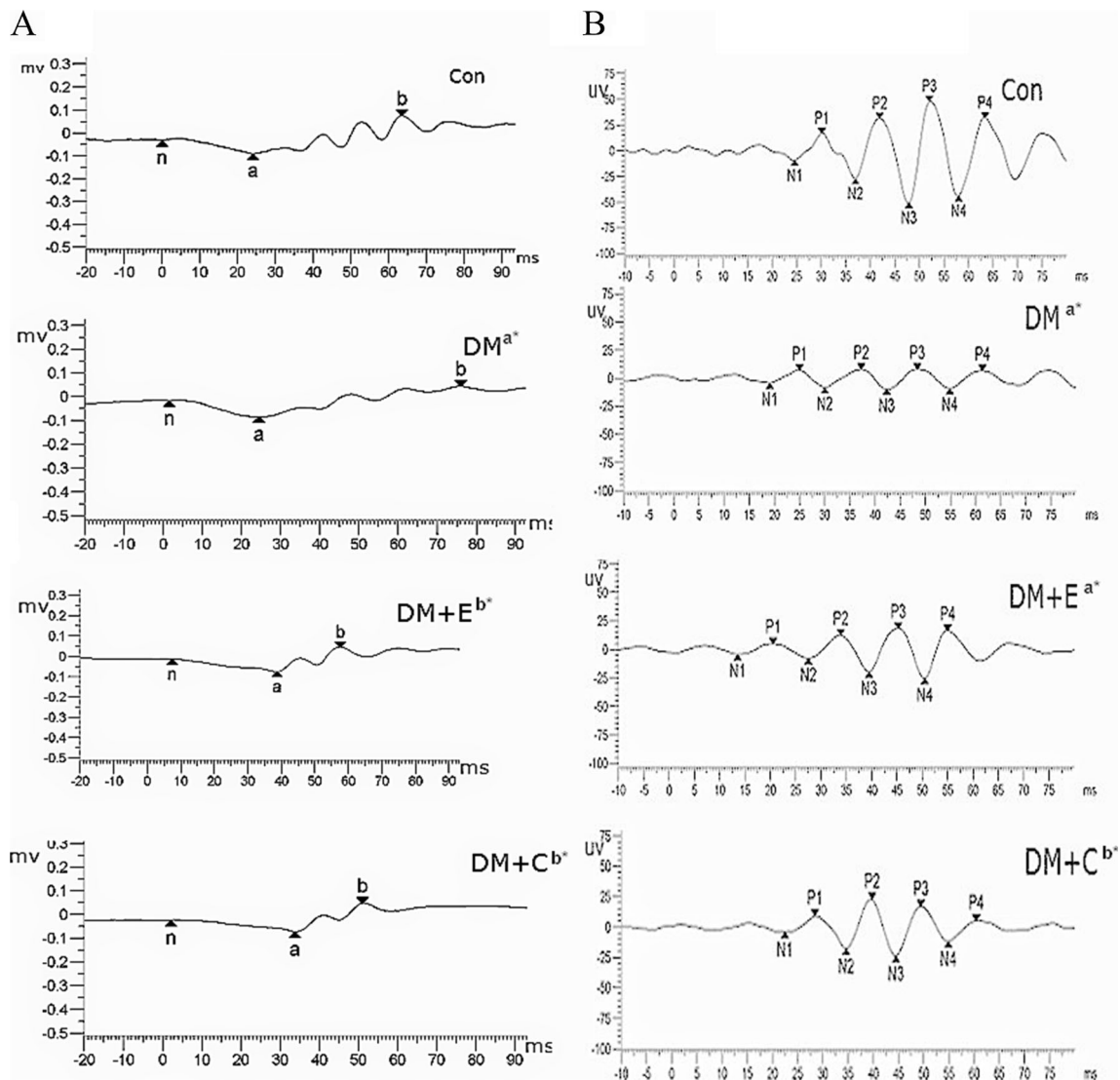


Fig. 5 Maximal responses and Ops of rat retinas after 4-week treatment. **a** Individual typical maximal responses recorded in each group. **b** Individual typical Ops recorded in each group, N: negative component,

P: positive component. * $p < 0.05$. ^a Compared with the CON group. ^b Compared with the DM group

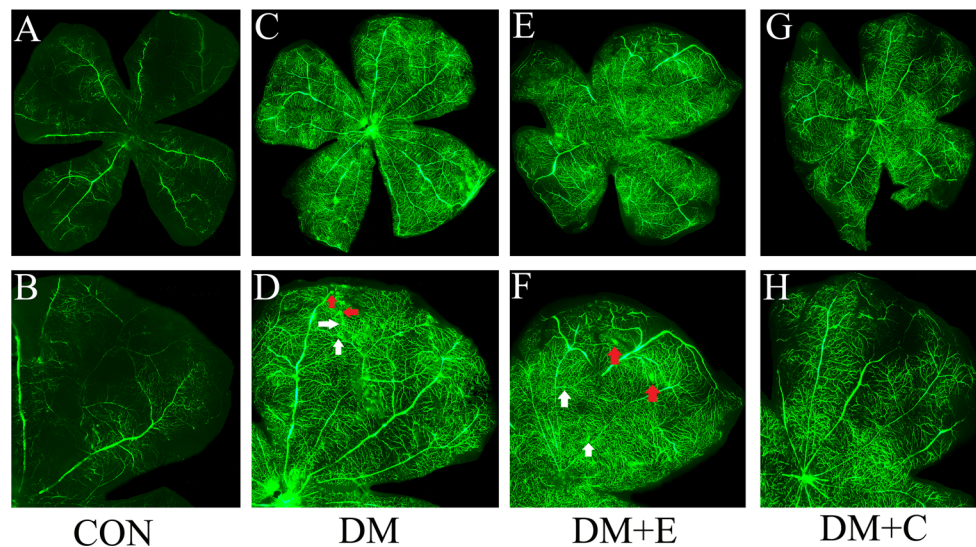


Fig. 6 Representative photographs of fluorescein retinal angiograms from each group of rats four weeks after treatment. **a, b** Clear and normally distributed vessels with no fluorescein exudation in the CON group. **c, d** Many microaneurysms and fluorescein exudation in the DM group. **e, f** Many microaneurysms and fluorescein exudation in the DM+

E group. **g, h** No obvious vascular exudation, distortion, or expansion in the DM+C group. *Top row*: whole retina montages created by many low-power field overlapping images; *bottom row*: a single image of the whole flat mount, showing one quadrant. *Red arrows*: fluorescein exudation; *white arrows*: microaneurysms

and reduces the structural damage in DR neural tissues in diabetic rats [10]. CEPO conferred neuroprotection in brain ischemic stroke, sciatic nerve compression, spinal cord injury, experimental autoimmune meningoencephalomyelitis, and diabetic neuropathy models [11]. In the present study, we verified that CEPO conferred the same protection in diabetic rats as EPO through an anti-apoptosis mechanism, and this provides a new option in DR treatment.

Although EPO conferred neuroprotection against DR, it induced retinal neovascularization and aggravated DR vasculopathy by binding to $(EPOR)_2$. Brines et al. [7] found that EPO exerted its neuroprotective function by binding with CD131. Our results demonstrate that in diabetic rats, CEPO administration increased CD131 expression, while EPO administration reduced it. CD131 is the co-receptor of granulocyte-macrophage colony-stimulating factor and interleukin-5, and its putative structure is similar to that of $(EPOR)_2$. Leist and colleagues [11] confirmed that CEPO had the same protective function in *N*-methyl-D-aspartate-induced apoptosis of hippocampal cells as EPO, but CEPO did not bind to $(EPOR)_2$. Based on our results and the above-mentioned studies, we speculate that CEPO may bind to CD131 to confer neuroprotection in DR. The reason CD131 expression was lower in diabetic rats after EPO treatment may be related to the receptor competition mechanism. When the rats received the same dose of EPO or CEPO, $(EPOR)_2$ bound competitively to EPO, resulting in a lower EPO dose that could bind to CD131. This mechanism would lead to a feedback response in CD131 expression. Furthermore, Livnah and colleagues [18] found that the affinity between EPO and CD131 was far lower than that between

EPO and $(EPOR)_2$. This also explains why CD131 expression was lower in diabetic rats after EPO treatment.

THY1 is a cellular surface protein in which glycosylated phosphatidylinositol anchors and is widely expressed in many cell types, including fibroblasts, ovarian cancer cells, endothelial cells, hematopoietic cells, and neuronal cells; it is also used as a surface marker of neuronal cells [19, 20]. Although THY1 expression is lower in the retina than in the central nervous system, it is the primary receptor of RGCs and is commonly used as a marker of RGCs [20, 21]. In the DR model, THY1 expression decreases as RGC apoptosis increases; therefore, quantification of THY1 expression can indirectly quantify RGC apoptosis. In our research, THY1 expression decreased in an obvious manner in diabetic rats and this was reflected in the reduced numbers of RGCs. This is in accordance with many previous studies [14–17]. However, after EPO or CEPO treatment, THY1 expression in the two groups also decreased slightly, demonstrating that the damage of so many retinal neural cells was irreversible despite the administration of retinal neuroprotective drugs.

Our results demonstrate that GFAP expression was highest in diabetic rats; after CEPO or EPO administration, GFAP expression was lower than that in untreated diabetic rats, but remained higher than that in the control rats. GFAP is the main cytoskeletal protein of astrocytes, and is usually used as an astrocyte and Müller cell surface marker [22, 23]. In the DR model, GFAP expression increased in an obvious manner along with abnormal activation of Müller cells [24]. Liu et al. [25] found that GFAP expression gradually increased over 4 days when they constructed a mouse periventricular leukomalacia model, peaking on the fourth day, and that

CEPO could not reduce GFAP expression as EPO did. DR is usually accompanied by abnormal activation of RGCs, which manifests as Müller cell activation and increased GFAP expression [24, 26]. This may explain why CEPO and EPO both cannot wholly inhibit Müller cell activation and why CEPO neuroprotection occurs mainly through the reduction of apoptotic RGCs.

VEGF-A may be a major direct intraocular neovascularization factor [27]. Thieme and colleagues [28] believed that VEGF-A could upregulate receptor numbers on the retinal vascular endothelial cell surface but not alter receptor affinity. VEGF-A can also increase microvascular permeability and damage the blood–retina barrier. Our research also confirmed the belief that VEGF-A expression is upregulated in an obvious manner in diabetic rats; moreover, VEGF-A expression was upregulated further after EPO administration. This may indicate that EPO itself upregulates VEGF-A expression, as it has been verified that EPO induces neovascularization via activation of the VEGF/VEGF2 and angiopoietin 1 (ANG1)/TIE2 receptor transduction pathways [29]. However, VEGF-A expression in diabetic rats after CEPO treatment was not as high as that after EPO treatment. As VEGF-A expression in the diabetic rats after CEPO treatment was not higher than that of untreated diabetic rats, we conclude that CEPO does not upregulate VEGF-A expression. Retinal microvessels in diabetic rats expanded to the point of microaneurysm, and fluorescein leakage was evident in the retinal microvessels, which was consistent with that of other studies [30–32]. The retinal microvessels in EPO-treated diabetic rats were similar to that of the untreated diabetic rats, and this may be due to the upregulated VEGF-A expression. Surprisingly, the retinal microvessels in CEPO-treated diabetic rats appeared the same as that of the control rats, and this may be because VEGF-A expression did not reach the threshold of neovascularization.

This study has two limitations. First, we did not examine a-wave change, which would have required a much longer time to observe. The a-wave mainly reflects the change in potential of the photoreceptor cells, while the main manifestation of DR is RGC apoptosis and abnormal activation of glial cells; detecting a-wave changes is not necessary [14–17]. Second, we did not investigate the CEPO–CD131 downstream signaling mechanism, and we will perform this study in the future.

In summary, we verified that CEPO treatment in DR through intraperitoneal injection can reach effective blood concentrations in retinal vessels and confers the same neuroprotective function as EPO, but does not inhibit hyperglycemia-induced Müller cell activation. CEPO may bind to CD131 instead of (EPOR)₂ to exert its neural anti-apoptotic function. Moreover, CEPO does not upregulate VEGF-A expression to induce neovascularization; thus, the side-effects in retinal microvessels caused by EPO can be avoided. This may be a new therapy for treating the many neural degeneration diseases in ophthalmology.

Acknowledgments This article is supported by Grant 30801269 from the National Natural Science Foundation of China.

Conflict of interest The authors declare that they have no conflict of interest.

Ethical standards Our animal studies have been approved by the appropriate ethics committee, and have therefore been performed in accordance with the ethical laid down in the 1964 Declaration of Helsinki and its later amendments.

References

1. Abbate M, Cravedi P, Iliev I et al (2011) Prevention and treatment of diabetic retinopathy: evidence from clinical trials and perspectives. *Curr Diabetes Rev* 7(3):190–200
2. Gutiérrez Manzanedo JV, Carral San Laureano F, García Domínguez G et al (2014) High prevalence of inactivity among young patients with type 1 diabetes in south Spain. *Nutr Hosp* 29(n04):922–928
3. Bringmann A, Pannicke T, Grosche J et al (2006) Müller cells in the healthy and diseased retina. *Prog Retin Eye Res* 25(4):397–424
4. Santiago AR, Cristóvão AJ, Santos PF et al (2007) High glucose induces caspase-independent cell death in retinal neural cells. *Neurobiol Dis* 25(3):464–472
5. Cheung N, Wong IY, Wong TY (2014) Ocular anti-VEGF therapy for diabetic retinopathy: overview of clinical efficacy and evolving applications. *Diabetes Care* 37(4):900–905
6. Jelkmann W (2013) Physiology and pharmacology of erythropoietin. *Transfus Med Hemother* 40(5):302–309
7. Brines M, Grasso G, Fiordaliso F et al (2004) EPO mediates tissue protection through an EPO and common beta-subunit heteroreceptor. *Proc Natl Acad Sci U S A* 101(41):14907–14912
8. Nangaku M (2013) Tissue protection by erythropoietin: new findings in a moving field. *Kidney Int* 84(3):427–429
9. King CE, Rodger J, Bartlett C et al (2007) EPO is both neuroprotective and neuroregenerative following optic nerve transection. *Exp Neurol* 205(1):48–55
10. Zhu B, Wang W, Qu Q et al (2008) EPO protects retinal neurons and glial cells in early-stage streptozotocin-induced diabetic rats. *Exp Eye Res* 86:375–382
11. Leist M, Ghezzi P, Grasso G et al (2004) Derivatives of EPO that are tissue protective but not erythropoietic. *Science* 305(5681):239–242
12. International Standardization Committee (1989) Standard for clinical electroretinography. *Arch Ophthalmol* 107(6):816–819
13. Junk AK, Mammis A, Savitz SI et al (2002) EPO administration protects retinal neurons from acute ischemia-reperfusion injury. *Proc Natl Acad Sci U S A* 99(16):10659–10664
14. Barber AJ, Gardner TW, Abcouwer SF (2011) The significance of vascular and neural apoptosis to the pathology of diabetic retinopathy. *Invest Ophthalmol Vis Sci* 52(2):1156–1163
15. Martin PM, Roon P, Van Eells RK et al (2004) Death of retinal in streptozotocin-induced diabetic mice. *Invest Ophthalmol Vis Sci* 45:3330–3336
16. Moore P, Elsherbey A, Room P et al (2001) Apoptosis cell death in the mouse retinal ganglion cell layer is induced in vivo by the excitatory amino acid homocysteine. *Exp Eye Res* 73(1):45–57
17. Park SH, Park JW, Park SJ et al (2003) Apoptotic death of photoreceptors in the streptozotocin-induced diabetic rat retina. *Diabetologia* 46:1260–1268
18. Livnah O, Stura EA, Middleton SA et al (1999) Crystallographic evidence for preformed dimers of erythropoietin receptor before ligand activation. *Science* 283(5404):987–990

19. Zhang XM, Li Liu DT, Chiang SW et al (2010) Immunopanning purification and long-term culture of human retinal ganglion cells. *Mol Vis* 16:2867–2872
20. Seki M, Nawa H, Morioka T et al (2002) Establishment of a novel enzyme-linked immune-sorbent assay for Thy-1; quantitative assessment of neuronal degeneration. *Neurosci Lett* 329(2):185–188
21. Nieto PS, Acosta-Rodríguez VA, Valdez DJ et al (2010) Differential responses of the mammalian retinal ganglion cell line RGC-5 to physiological stimuli and trophic factors. *Neurochem Int* 57(3):216–226
22. Middeldorp J, Hol EM (2011) GFAP in health and disease. *Prog Neurobiol* 93:421–443
23. Yanguas-Casás N, Barreda-Manso MA, Nieto-Sampedro M et al (2014) Tauroursodeoxycholic acid reduces glial cell activation in an animal model of acute neuroinflammation. *J Neuroinflammation* 11(1):50
24. Lieth E, Barber AJ, Xu B et al (1998) Glial reactivity and impaired glutamate metabolism in short-term experimental diabetic retinopathy. Penn State Retina Research Group. *Diabetes* 47(5):815–820
25. Liu W, Shen Y, Plane JM et al (2011) Neuroprotective potential of erythropoietin and its derivative carbamylated erythropoietin in periventricular leukomalacia. *Exp Neurol* 230(2):227–239
26. Ly A, Yee P, Vessey KA et al (2012) Early inner retinal astrocyte dysfunction during diabetes and development of hypoxia, retinal stress, and neuronal functional loss. *Invest Ophthalmol Vis Sci* 52(13):9316–9326
27. Chen N, Wang J, Hu Y et al (2014) MicroRNA-410 reduces the expression of vascular endothelial growth factor and inhibits oxygen-induced retinal neovascularization. *PLOS ONE* 9(4):e95665
28. Thieme H, Aiello LP, Takagi H et al (1995) Comparative analysis of vascular endothelial growth factor receptors on retinal and aortic vascular endothelial cells. *Diabetes* 44(1):98–103
29. Sun Y, Calvert JW, Zhang JH (2005) Neonatal hypoxia/ischemia is associated with decreased inflammatory mediators after erythropoietin administration. *Stroke* 36:1672–1678
30. Luty GA (2013) Effects of diabetes on the eye. *Invest Ophthalmol Vis Sci* 54(14):ORSF81–ORSF87
31. Lombardo M, Parravano M, Serrao S et al (2013) Analysis of retinal capillaries in patients with type 1 diabetes and nonproliferative diabetic retinopathy using adaptive optics imaging. *Retina* 33(8):1630–1639
32. Giocanti-Auregan A, Tadayoni R, Ahn L et al (2013) Mouse models of diabetic retinopathy: systematic review of the literature. *J Fr Ophthalmol* 36(3):268–276